Crystallization kinetics of poly(*p*-phenylene sulphide): the effect of branching agent content and endgroup counter-atom

Leonardo C. López and Garth L. Wilkes*
Department of Chemical Engineering, Polymer Materials and Interfaces Laboratory, Virginia Polytechnic Institute and State University, Blacksburg, VA 24061, USA

and Jon F. Geibel
Phillips Petroleum Company, Research and Development, Bartlesville, OK 74004, USA
(Received 14 March 1988; revised 9 June 1988; accepted 18 June 1988)

The crystallization behaviour of poly(phenylene sulphide) (PPS) has been studied as a function of branching agent (trichlorobenzene) concentration in polymerization, and as a function of the chemical nature of the endgroup counter-atom. In both cases, the bulk crystallization phenomena could be described by the Avrami equation with exponent $n \approx 3$. An increase of the branching agent concentration in polymerization caused decreases of the linear crystal growth rate, overall rate of bulk crystallization, nucleation density, and heat of crystallization. The effect of branching on the linear crystal growth rate seemed to be more important than that of molecular weight. The chemical nature of the endgroup counter-atom affected the kinetic parameters in different ways. The endgroup counter-atoms considered were hydrogen, calcium, zinc and sodium. In decreasing order, the crystal growth rates were found to be PPSCa > PPSH > PPSZn > PPSNa. However, the overall rates of bulk crystallization and the estimated nucleation densities followed the order PPSH > PPSZn > PPSCa > PPSNa. The nucleation densities accounted for the different rates of bulk crystallization. The crystallinity content of PPSH seemed to be lower than those of PPSZn, PPSCa, and PPSNa. While the lower crystallinity content of PPSH could be rationalized by considering the ionic character of the endgroups, it was not possible to account systematically for the nucleation and growth rate dependencies on the nature of the endgroup counter-atom.

(Keywords: poly(*p*-phenylene sulphide); crystallization; crystallization kinetics)

INTRODUCTION

The traditional synthetic process to prepare poly(phenylene sulphide) (PPS) involves the reaction of *p*-dichlorobenzene with sodium sulphide in a polar solvent[1]. The mechanism consists of a series of nucleophilic displacement reactions that lead to the formation of polymer and production of sodium chloride as by-product. This method produces a linear polymer of low molecular weight in the range 15 000–20 000 Daltons. This molecular weight can be increased by a 'curing' process that causes chain extension, branching and some degree of crosslinking[2,3]. The curing process may be conducted in the melt or in the solid state just below the melting point of PPS ($\approx$285°C) in the presence of air. The extent of 'curing' may be controlled through the residence time and reaction temperature[4].

At a later time, a new process was developed which allows the synthesis of higher molecular weight PPS directly during the polymerization[5]. This process comprises the preparation of sodium sulphide from aqueous sodium hydrosulphide and sodium hydroxide in a polar solvent that contains an alkali–metal carboxylate; after water removal, this mixture is reacted with *p*-dichlorobenzene in a polar solvent at high temperature. The alkali-metal salt apparently 'moderates' the polymerization process, presumably by reacting with sodium sulphide to form the species that initiates the polymerization reaction. Since the PPS polymerization is based upon anionic nucleophilic reactions, one might expect ionic endgroups to be present. In view of the work of Legras *et al.*[6] and Bailly *et al.*[7] on the influence of ionic endgroups on the crystallization behaviour of bisphenol-A polycarbonate and poly(ethylene terephthalate), a systematic investigation of the effect of the endgroup counter-atom on the kinetics of crystallization of PPS is addressed as one aspect of this paper.

Hill[8] stated that the molecular weight of PPS can be increased further during polymerization by the addition of small amounts of 1,2,4-trichlorobenzene (TCB), producing a lightly branched polymer (long branches) with molecular weight that can reach the order of 200 000. The introduction of branches has been shown to influence the crystallization behaviour of polyethylene, not only with regard to the morphology[9–13], but also the kinetics of crystallization[14–16]. For example, Voigt-Martin *et al.*[13] observed that the lateral dimensions of lamellae in hydrogenated polybutadiene became smaller as the branch content increased. An increase in the ethyl-branch content from 2.2 mol% to 3.2 mol% produced a decrease of the crystallite thickness from 7 to 4 nm. Further increase in the branch content to 4.5 and 5.7 mol% produced small crystallites that did not present the lamellar characteristics. In the case of the kinetics of bulk crystallization, it has been shown that low density polyethylene (short branches) presents crystallization isotherms which cannot be explained in terms of a simple

* To whom correspondence should be addressed

0032-3861/89/010147-09$03.00

Table 1 Characteristics of samples utilized to study the effect of branching agent content on the crystallization kinetics of PPS

Sample designation	TCB content (mol%)	$\langle M_w \rangle$	$\langle M_w \rangle / \langle M_n \rangle$
PPS00	0	63000	1.5
PPS13	0.13	75000	1.5
PPS20	0.20	65000	1.7

Avrami equation[14–16]. Moreover, Strobl, Schneider and Voigt-Martin[17] proposed a model to explain some of these effects in LLDPE by considering that branch points remained in the amorphous interlamellar layers, and that the distribution of branch points was one of the important controlling factors of the kinetics of crystallization. An important point worth considering is the difference between LLDPE and PPS studied in the present Paper. LLDPE presents short side-chains, such as ethyl, butyl, and hexyl groups. However, branched PPS synthesized by the addition of small amounts of 1,2,4-trichlorobenzene in polymerization produces long branches. Consequently, different crystallization behaviour might be expected from that of LLDPE.

In previous studies, the authors of this paper have reported on the morphological textures of PPS[18], and on the kinetics of crystallization of PPS as a function of molecular weight[19]. Continuing the studies on the crystallization behaviour of PPS, the present work describes the effects of addition of trichlorobenzene (branching agent) and the nature of the endgroup counter-atom on the kinetics of crystallization of PPS.

EXPERIMENTAL

Three samples of PPS were kindly donated by Dr C. J. Stacy of Phillips Petroleum Co. to study the effect of branching agent. The sample nomenclature and characteristics are shown in *Table 1*. PPS is known for its excellent chemical resistance. Due to this excellent chemical resistance, and insolubility in solvents below 200°C, a high temperature gel permeation chromatography technique has recently been developed to determine molecular weight distributions[20]. Furthermore, the high insolubility of PPS has precluded, to date, the study of the branching characteristics by conventional techniques such as nuclear magnetic resonance. Therefore, the trichlorobenzene (TCB) content in the reaction vessel is utilized to characterize the concentration of branches in the polymer. This implies a linear relation between TCB content and branch concentration.

The similar molecular weight and molecular weight distribution of samples PPS00 and PPS20 allow the investigation of the effect of TCB content on the kinetics of crystallization with a very small contribution by the effect of molecular weight. In contrast, polymer PPS13 will present the mixed effects of branching and molecular weight differences.

The specimens utilized to study the 'endgroup' effect were prepared by an effective ion-exchange procedure that presumably takes place at the endgroups of the polymer, as follows. One lot of high molecular weight linear PPS was utilized for the ion exchange procedures. Selectively introducing a specific metal counter ion to the polymer requires rigorous removal of all other metal ions normally present in the polymer. An efficient method to remove residual metal ions from PPS involves charging the PPS and a dilute solution of acetic acid (1%, v:v) to a stainless steel autoclave. The reaction mixture was degassed by pressurizing to 200 psig (13.7 MPa) with nitrogen and then releasing the pressure. This pressurization/release cycle was repeated six times. Degassing in this manner eliminates oxygen from the autoclave and minimizes the possibility of adventitious oxidative chain extension. The reaction mixture was then heated to 235°C with agitation and held at that temperature for one hour. The polymer slurry was then cooled and filtered and the recovered polymer was washed with glass-distilled water at room temperature to remove any residual adsorbed acetic acid solution. A sample of the acid washed polymer was analysed for residual metal ions. To introduce specific metal ions to the polymer, an aliquot of the acid-washed polymer was charged to the autoclave along with a dilute metal acetate solution (1%, w:v). Degassing was accomplished as previously described. The reaction mixture was heated to 235°C for 30 min and cooled and the polymer recovered as described above. All samples of PPS were dried in a vacuum oven at 100°C before analysis. *Table 2* summarizes the samples, their designation and metal analyses obtained by plasma emission spectroscopy of acid digestates of residual polymer ash. Using such a method to prepare the polymer samples allows one to avoid the effect of molecular weight, since the same PPS is ion-exchanged. However, the procedure inherently produces samples that have higher nucleation densities, as will be shown below.

GROWTH RATE MEASUREMENTS

PPS specimens were moulded into thin films between glass cover slips to measure spherulitic growth rates. A Zeiss polarizing microscope equipped with a Leitz 350 heating stage and a 35 mm camera was used. Temperature calibration of the heating stage was performed with naphthalene, indium, anthraquinone and sodium nitrate.

PPS is known to undergo chemical reactions at high temperature in the presence of oxygen that involve chain extension, branching and some degree of crosslinking[3]. These reactions alter the molecular weight and architecture of PPS. Therefore, the residence times of samples at high temperature need to be minimized. Moreover, the crystallization studies must be conducted under a nitrogen atmosphere to reduce to a minimum the extent of these reactions. For this reason, the samples were held at 320°C for 4 min before crystallization. Crystallizations were performed in the temperature range

Table 2 Sample designation and analyses for PPS specimens used to study the effect of the nature of the endgroup counter-atom

Sample designation	Counter-atom	Metal analyses (ppm)		
		Ca	Na	Zn
PPS as received	–	786.0	77.3	20.3
PPSH	Hydrogen	15.7	BDL[a]	BDL
PPSZn	Zinc	BDL	BDL	1950.0
PPSCa	Calcium	417.0	BDL	54.4
PPSNa	Sodium	9.0	268.0	24.7

[a] Below detection limits

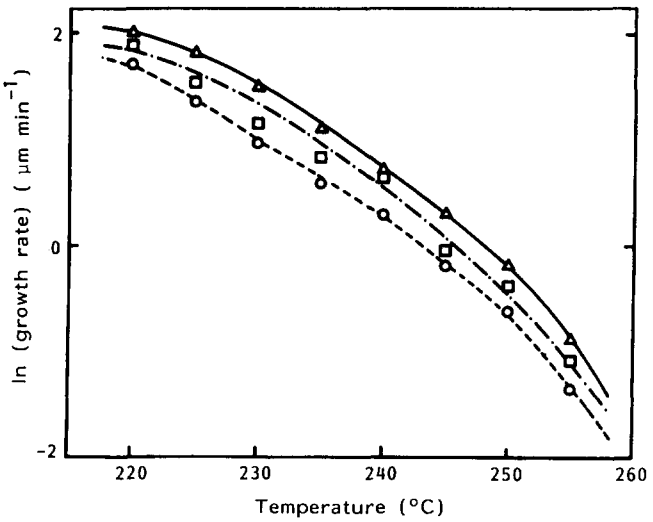

Figure 1 Relationship between crystal growth rate and crystallization temperature for PPS samples crystallized from the melt as a function of the branching agent content. Δ, ——, $\bar{M}_w = 63\,000$, TCB = 0 mol%; □, —·—, $\bar{M}_w = 75\,000$, TCB = 0.13 mol%; ○, – – –, $\bar{M}_w = 65\,000$, TCB = 0.20 mol%

220–260°C, minimizing the residence times of the samples at high temperatures as much as possible. No crystallization time was longer than 60 min.

Spherulite growth was followed by taking photographs with a 35 mm camera at fixed time intervals. The spherulite diameters were measured from these optical micrographs. The crystal growth rates were determined by plotting spherulitic radius as a function of time and determining the slope of the straight lines. Reproducibility of the growth rate measurements indicated a percentage deviation $< 10\%$.

RATE OF BULK CRYSTALLIZATION

A Perkin–Elmer DSC-4 differential scanning calorimeter was used to obtain bulk crystallization isotherms. The temperature calibration was performed with an indium standard and anthraquinone. The PPS samples were weighed in aluminium pans (2–3 mg) and were crystallized from the melt after being held at 320°C for 4 min.

Crystallization from the melt was only possible in the temperature range 220–260°C. Two factors contributed to limit this temperature range. The upper end was set by the long residence time needed to complete crystallization at high temperatures, which may induce chemical reactions, as discussed before. The lower limit was imposed by the high nucleation densities encountered. For this reason, the cooling rates available in the DSC-4 were not suffficiently fast to permit the achievement of temperatures lower than 220°C before the initiation of crystallization. This latter limitation was more critical for the samples used to study the effect of endgroup counter-atom.

To obtain crystallization data in the diffusion controlled part of the crystallization rate–temperature curve, thin amorphous PPS films were formed. These were prepared by compression moulding PPS at 320°C for 4 min at 2000 psi (13.7 MPa), and quenching in ice water. Similarly to crystallization from the melt, the temperature range for crystallization from the glassy state was very limited.

The thermodynamic melting points of samples containing trichlorobenzene were determined by the method of Hoffman and Weeks[21]. The method consists of crystallizing polymer samples at selected supercoolings. Then the experimental melting points are determined and plotted as functions of the crystallization temperature. At the higher crystallization temperatures, a straight line relationship between melting and crystallization temperatures is found. This line is extrapolated to $T_c = T_m$, and this point represents the thermodynamic melting point T_m^0.

DATA ANALYSIS

The overall rate of bulk crystallization was analysed in terms of the well known Avrami equation[22]

$$x_c(t) = 1 - e^{-Kt^n} \tag{1}$$

In this equation, $X_c(t)$ is the volume fraction of crystals at time t; K is a rate constant that includes the temperature dependent terms, and contains information regarding growth and nucleation rates; and n, the Avrami exponent, is a constant dependent on the types of processes occurring during nucleation and growth. Assuming that nucleation results in three-dimensional spherulites, and that the increase in crystal dimensions is linear with crystallization time, the nucleation density N (number of nuclei per cubic centimetre) can be estimated by

$$N = 3K/4\pi G^3 \tag{2}$$

where K is obtained from equation (1) and G is the linear crystal growth rate. Therefore, the combination of K obtained from differential scanning calorimetry (d.s.c.) experiments, and G obtained from polarized light

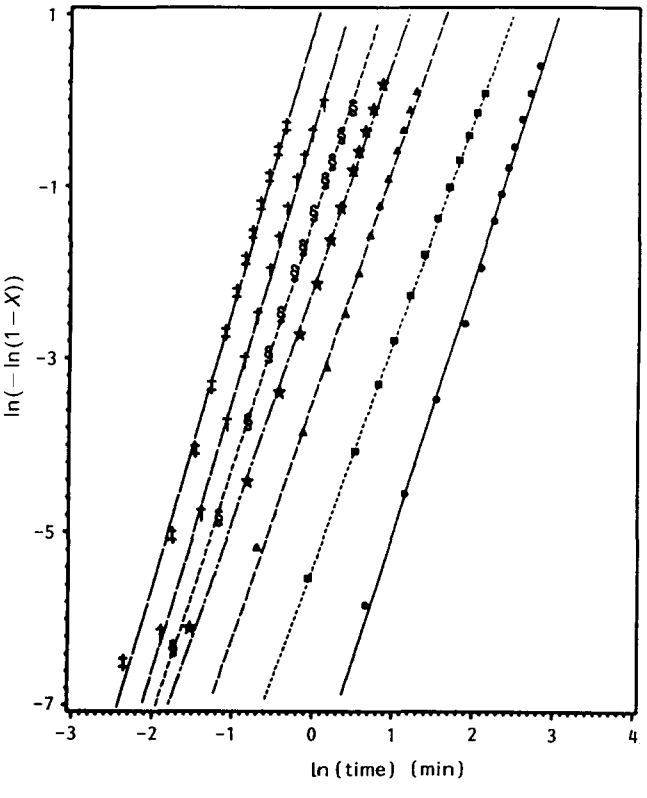

Figure 2 Double logarithmic plot of amorphous content *versus* ln(time) following the Avrami equation corresponding to PPS20. T_c (°C): ●, 250; ■, 245; ▲, 240; ★, 235; §, 230; †, 225; ‡, 220

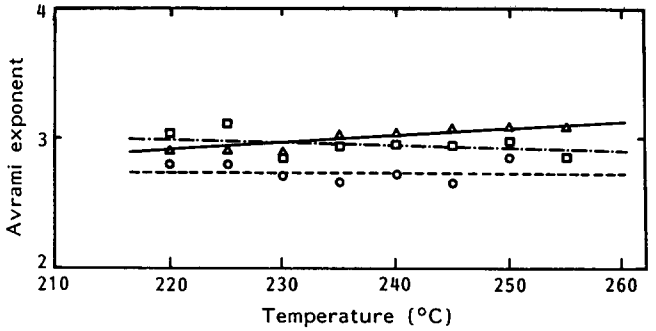

Figure 3 Avrami exponent as a function of crystallization temperature for PPS crystallized from the melt. For meaning of symbols see *Figure 1*

microscopy experiments on spherulitic growth rates allows the estimation of the nucleation density as a function of crystallization temperature.

The parameters in equation (1) were determined by methods described in a previous paper concerned with the effect of molecular weight on the kinetics of crystallization of PPS[19]. A plot of the double logarithm of the amorphous content as a function of the logarithm of time allows the determination of K from the calculated intercept, and n from the slope of the straight line. In addition, the crystallization half-time method was used to determine these parameters[23]. It involves the determination of the crystallization halftime, $t_{1/2}$, from a graph of the amorphous content as a function of time, and the calculation of the slope, S, of the curve of amorphous content as a function of logarithm of time at time $= t_{1/2}$. The parameters K and n are calculated by means of the following equations

$$K = \frac{\ln 2}{t_{1/2}^n} \tag{3}$$

$$S_{t_{1/2}} = \frac{n \ln 2}{2} \tag{4}$$

RESULTS AND DISCUSSION

Effect of branching agent

Linear crystal growth rate data obtained via polarizing optical microscopy are presented in *Figure 1* as plots of the logarithm of growth rate *versus* crystallization temperature. Slower crystal growth rates are observed as the trichlorobenzene content increases, i.e. as the concentration of branches increases. Quantitatively for PPS, the crystal growth rates decreased by a factor of 2.2 when the TCB content increased from 0 to 0.2 mol%. Since the molecular weights of samples PPS00 and PPS20 are very similar, the decrease in the crystal growth rate is fully attributed to the long branches introduced upon the addition of TCB in polymerization. An intermediate value of the TCB content (0.13 mol%) produces the lowering of the growth rate by a factor of 1.4. However, polymer PPS13 has a higher molecular weight than PPS00. Consequently, PPS13 presents contributions due to branching and possibly due to a slightly different molecular weight. However, the contribution of the molecular weight to the lowering of the crystal growth rate can be estimated if it is assumed that branched PPS follows the same molecular weight dependence as linear PPS. It was shown in previous work[19] that the crystal growth rate of linear PPS followed a logarithmic function of the number average molecular weight,

$$\ln G = b \ln \langle M_n \rangle + a \tag{5}$$

Considering the effect of molecular weight on G, and taking values for b and a from reference 19, a crystal growth rate of 2.98 μm min^{-1} is estimated for PPS13 at a supercooling of 70°C. Growth rate data extracted from *Figure 1* gives $G = 3.32$ μm min^{-1} for PPS00, and $G = 2.36$ μm min^{-1} for PPS13 at a supercooling of 70°C. Comparison of these results indicates that the molecular weight contribution to the lowering of the growth rate is only one fourth of the total decrease. Therefore, the effect of branching on the growth rate seems to be far more important than that of molecular weight for PPS13. Although crystal growth rate and lamellar thickness cannot be directly related, it is interesting to note that Maderek and Strobl[15] concluded that branching had a larger effect on the lamellar thickness of LLDPE (short branches) than molecular weight and molecular weight distribution. These authors found that the lamellar thickness (d_c) of fractions remained constant as the viscosity average molecular weight changed from 20 000 to 80 000. Furthermore, d_c was the same for fractions and for unfractionated polymer. That is, the contributions of molecular weight and molecular weight distribution to the crystallization behaviour of LLDPE were negligible.

Figure 2 presents an Avrami plot, corresponding to PPS20, i.e. a plot of $\ln[-\ln(1-X_c(t))]$ *versus* logarithm of time. This plot shows that the d.s.c. data corresponding to PPS20 follow almost perfectly an Avrami equation for the overall rate of bulk crystallization. *Figure 3* displays the values of the Avrami exponent (n) as a function of the crystallization temperature corresponding to samples crystallized from the melt. The values of n are all very close to 3. This behaviour contrasts with that found for

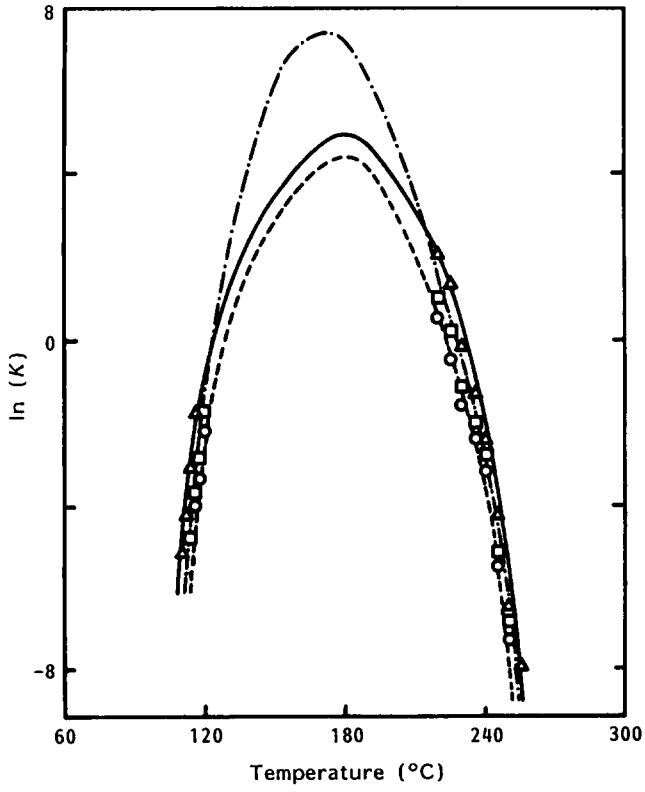

Figure 4 Relationship between rate constant, K, and crystallization temperature. For meaning of symbols see *Figure 1*

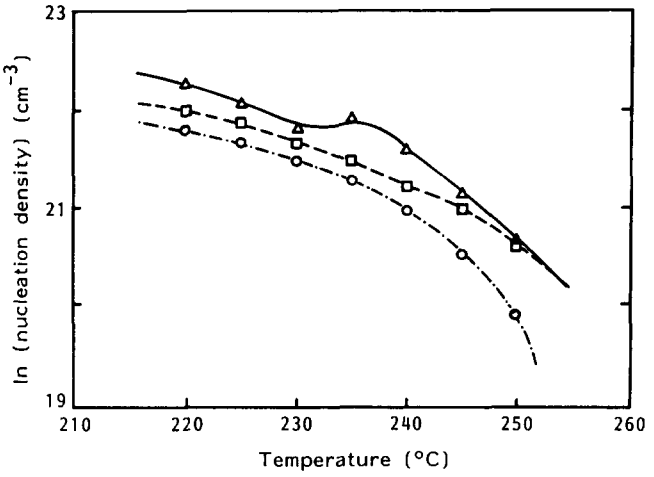

Figure 5 Graph of nucleation density as a function of crystallization temperature. For meaning of symbols see *Figure 1*

LLDPE[14]. In LLDPE, the overall rate of bulk crystallization could not be interpreted by a single Avrami equation. In addition, the Avrami exponents derived from crystallization isotherms of LLDPE took on unusually low values, as low as $n \approx 1$. However, as expressed in the Introduction, there is an important difference between the topology of LLDPE and PPS studied in this paper. The PPS samples analysed in the present paper have long branches, as opposed to short ones in LLDPE. Therefore, a different behaviour of the overall rate of bulk crystallization might well be expected.

Figure 4 shows plots of the logarithm of K as a function of the crystallization temperature. As expressed in the Experimental section, there were limitations in the temperature ranges studied. Due to the start of rapid crystallization before temperature stabilization, no reliable data points could be gathered in the region of fast crystallization rates. Therefore, the curves were constructed following a third-order polynomial regression. The rate maxima are located in the range 170–180°C, in agreement with values previously reported for linear PPS[19,24,25]. At a supercooling of 75°C, the overall rate of bulk crystallization, K, decreases by a factor of 2 as the TCB content varies from 0 to 0.13 mol%, and by a factor of 5 as TCB content changes to 0.20 mol%. The crystallization half-time varies accordingly. There is an increase in $t_{1/2}$ by a factor of 1.8 as the TCB content increases to 0.13 mol%. Further increase of TCB concentration to 0.20% by weight produces an increase in $t_{1/2}$ by a factor of 4. These factors are higher than those found for the linear crystal growth rate, especially for sample PPS20, indicating a more important effect of branching on the overall rate of bulk crystallization than on the linear crystal growth rate. Consequently, the results seem to indicate that nucleation density is playing an important role. *Figure 5* is a graph of the logarithm of nucleation density as a function of the crystallization temperature calculated by means of equation (2) for PPS with different trichlorobenzene contents. The nucleation density of PPS13 is only 25% lower on average than that of PPS00. However, PPS20 shows nucleation densities that are lower than those of PPS00 by 350%. These values indicate that the concentration of branching agent, trichlorobenzene, not only affects the crystal growth rate but also the nucleation density.

Figure 6 shows a graph of the normalized overall heat of crystallization as a function of T_c for PPS crystallized from the melt. The heat of crystallization presents the usual increasing trend with increasing crystallization temperature. PPS00 and PPS13 have very similar values of ΔH_c. However, PPS20 displays slightly lower values at higher crystallization temperatures, indicating that the crystalline content of branched PPS is lower than that of linear PPS. Furthermore, the perfection of the crystalline phase in branched PPS is not as high as that of linear PPS. This is reflected by the values of the equilibrium melting temperatures determined in *Figure 7*. Linear PPS presents a T_m^0 of 312°C, 3°C lower than the value reported by Lovinger *et al.*[25]; PPS13 has a T_m^0 of 304°C, and PPS20 (with higher concentration of branches) shows a T_m^0 of 301°C. A similar monotonic decrease of measured melting temperatures with increasing branch concentration was observed in LLDPE by Mandelkern and Maxfield[11]. The equilibrium melting temperature is an indication of the perfection of the crystals formed. Higher melting points indicate higher perfection of the crystals. Therefore, perfection of the crystals decreases as the TCB content increases in PPS. Since the branch points would not fit in the crystal lattice, they would cause disruption of the crystal order and a decrease of the crystalline content. Kawai *et al.*[12] found results supportive of this argument when studying solution grown crystals of alkyl-branched polyethylene by X-ray diffraction. These authors indicated that the overall amorphous fraction found on solution grown crystals of branched polyethylene was larger than that of linear polyethylene. In addition, the same authors reported that the branches seemed to concentrate in the amorphous fraction of crystals and within the crystal defects. Voigt-Martin *et al.*[13] reported that in hydrogenated polybutadienes (ethyl branched samples) the lamellar structure deteriorates as the concentration of branches increases. This deterioration produces the disappearance of the lamellar character at a concentration of 4.5 mol% of ethyl branches. Furthermore, at the same molecular weight, a branched polymer has more chain ends per molecule,

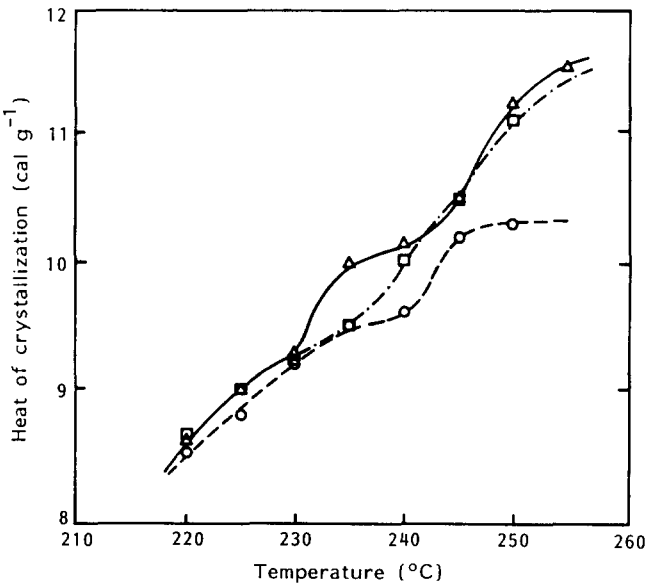

Figure 6 Heat of crystallization as a function of crystallization temperature for PPS crystallized from the melt. For meaning of symbols see *Figure 1*

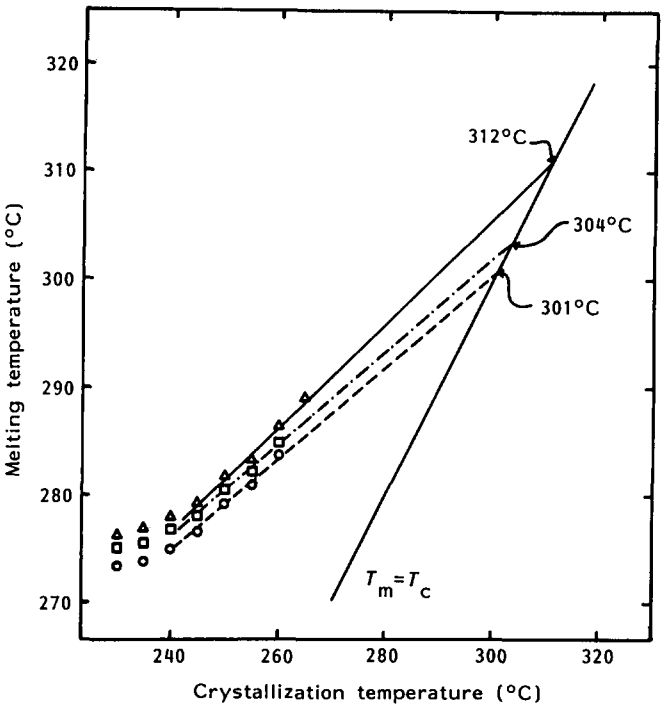

Figure 7 Hoffman–Weeks plots used to determine the thermodynamic melting points of PPS with different trichlorobenzene contents. For meaning of symbols see *Figure 1*

which will contribute to lower the crystallinity content. Therefore, it seems reasonable to expect lower values of the heat of crystallization for PPS with higher trichlorobenzene content.

Effect of endgroup counter-atom

Figure 8 presents the linear crystal growth rate data corresponding to PPS with different endgroup counter-atoms. Although the effect of the counter-atom is small, the small percentage deviation in the growth rate reproducibility indicates that the different G values are significant. The decreasing order of linear crystal growth rates is calcium > hydrogen > zinc > sodium. At this point, this ordering of the crystal growth rates is not fully understood. One might argue that there is a molecular weight increase due to chain extension by means of the ionic endgroups. In this respect, a highly electropositive cation would be suspected of causing a more important effect. For example, sodium would form strong ionic bonds with the phenoxide endgroups. Similarly, calcium would also be able to form strong ionic bonds. Furthermore, since calcium is divalent, it might be able to cause chain extension to a greater degree than sodium, producing slower crystal growth rates. However, PPSNa presents the lowest crystal growth rates and PPSCa shows the fastest crystal growth rates. Therefore, such an argument is not a plausible explanation of the crystal growth rates observed. Quantitatively, the crystal growth rates corresponding to PPSCa are on average twice those of PPSNa. Similarly, PPSH has growth rates 1.6 times faster than PPSNa, and crystal growth rates corresponding to PPSZn are 1.4 times faster than those of PPSNa. However, the growth rates of PPSNa and those of the as received PPS are about the same[19]. Since crystal growth rates depend on both the transport and the secondary nucleation events occurring during crystallization, the data indicate that one or both processes is affected in the case of PPS containing calcium, hydrogen and zinc counter-atoms. While we would suggest it is likely that the nucleation features are influenced, we have no further support of this speculation at this time.

The Avrami plot in *Figure 9* indicates that the d.s.c. data follow very well an Avrami equation for the overall rate of bulk crystallization. *Figure 10* presents the values of the Avrami exponent, n, as a function of the crystallization temperature. The values of n are all near 3, except for PPSH, which has lower values, of the order of 2.6. These lower values may be attributed to growth that is not three-dimensional. However, polarized optical microscopy studies did not show evidence of non-spherulitic superstructure.

Figure 11 displays a plot of the logarithm of K as a function of the crystallization temperature corresponding to PPSH and PPSNa as an example. By following a third-order polynomial, the rate maxima are found at 180°C, in agreement with values reported previously[19,24,25]. The overall rate of bulk crystallization is also affected by the nature of the endgroup counter-atom. However, the order of decreasing K is different from that observed for the crystal growth rates. The decreasing order is PPSH > PPSZn > PPSCa > PPSNa. PPSNa remains the slowest crystallizing polymer. PPSCa has values of overall rate of bulk crystallization 1.6 times those of PPSNa; K corresponding to PPSZn is 2.1 times that of PPSNa; and PPSH presents an overall rate of bulk crystallization that is 17 times faster than that of PPSNa! Similarly, the crystallization half-times of PPSH and PPSNa have corresponding trends. In addition, the values of K corresponding to PPSNa are, on average, 65 times those of PPS that has not undergone the ion-exchange process.

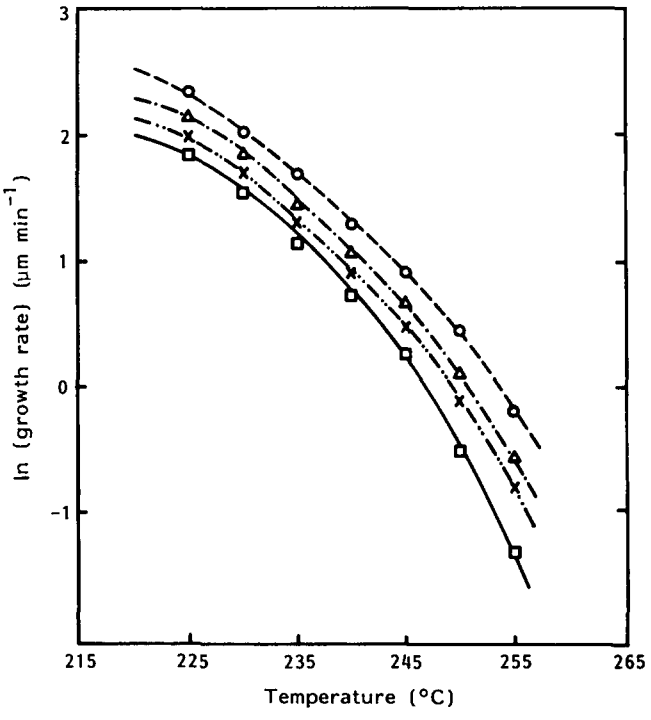

Figure 8 Relationship between crystal growth rate and crystallization temperature for PPS crystallized from the melt as a function of the chemical nature of the endgroup counter-atom: □, ——, Na; ○, – – –, Ca; △, —·—, H; ×, —··—, Zn

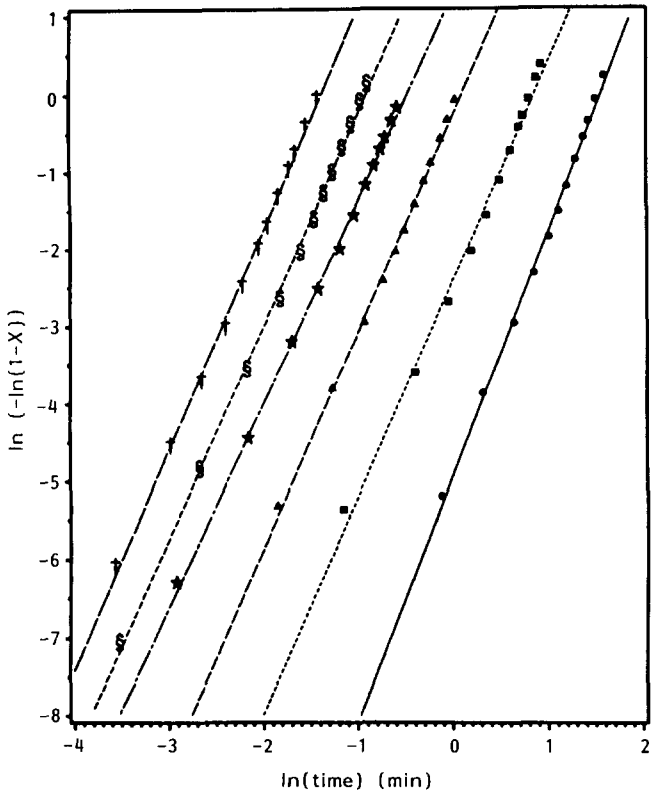

Figure 9 Double logarithmic plot of amorphous content *versus* ln(time) following the Avrami equation corresponding to PPSH. T_c (°C): ●, 255; ■, 250; ▲, 245; ★, 240; §, 235; †, 230

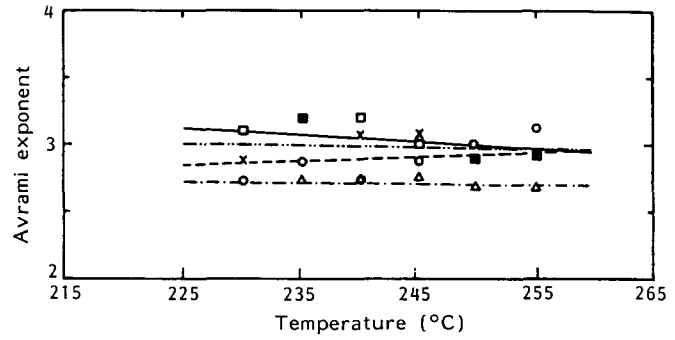

Figure 10 Avrami exponent as a function of the crystallization temperature for PPS with different endgroup counter-atoms crystallized from the melt. For meaning of symbols see *Figure 8*

Since the linear crystal growth rates are about the same for these two polymers, the data on overall rate of bulk crystallization suggest that *nucleation density is playing a very important role* due to the exchange procedure. Indeed, this is the case. *Figure 12* shows plots of the logarithm of nucleation density as a function of crystallization temperature for samples crystallized from the melt. The nucleation density corresponding to PPSNa is 20 times that of PPS that has not undergone the ion-exchange processes. Furthermore, the nucleation density of PPSNa remains fairly constant in the range of temperature studied. PPSH presents the highest nucleation density, about 8 times that of PPSNa. PPSZn and PPSCa have nucleation densities lower than that of PPSNa, with PPSCa the lowest. Therefore, the nucleation density determines the rate of bulk crystallization and not the crystal growth rate. Such an important effect of ionic endgroups on the nucleation density was previously observed in sodium carboxylate-terminated poly(ethylene terephthalate) (PET)[6], and sodium phenoxide-terminated bisphenol-A polycarbonate (PC)[7]. Legras *et al.*[6] indicated that the ionic end-groups of PET were aggregated in a separate

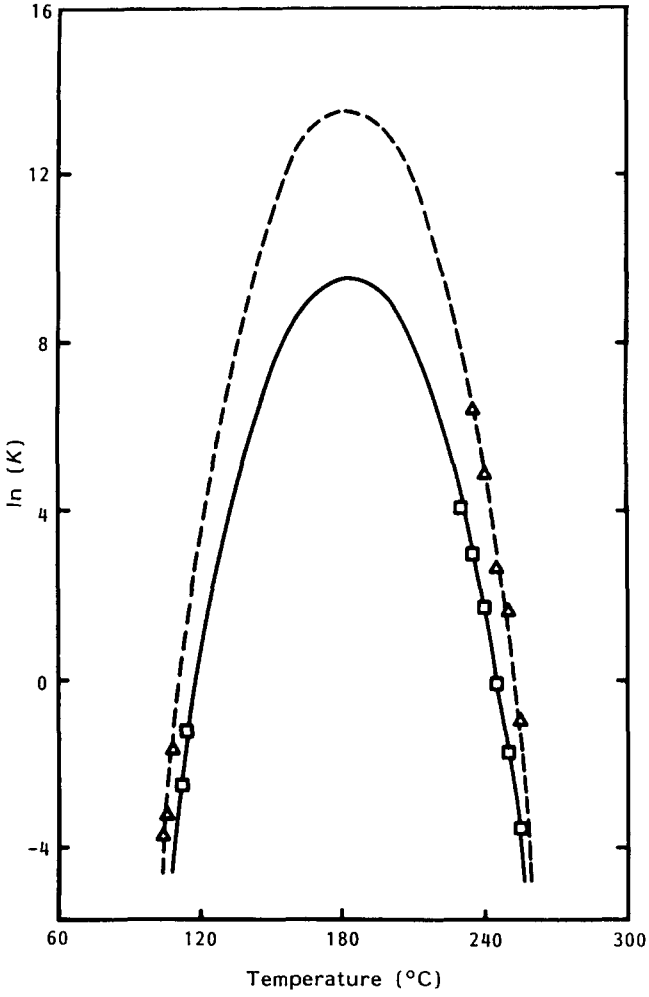

Figure 11 Relationship between rate constant K and crystallization temperature. □, ——, Na; △, – – –, H

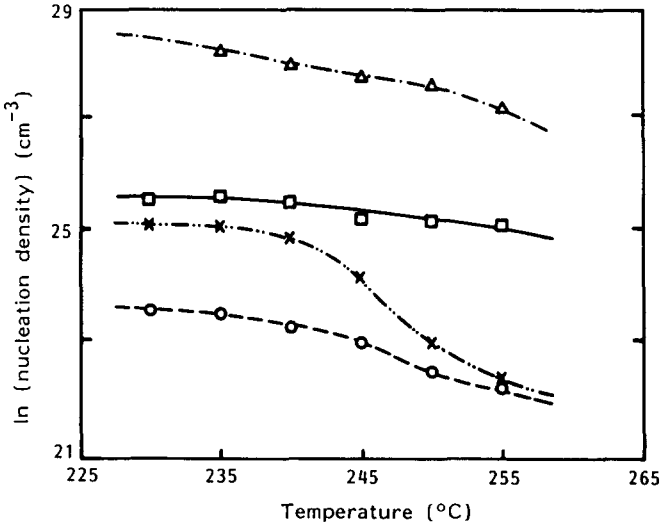

Figure 12 Plot of nucleation density as a function of the crystallization temperature as calculated by equation (2). For meaning of symbols see *Figure 8*

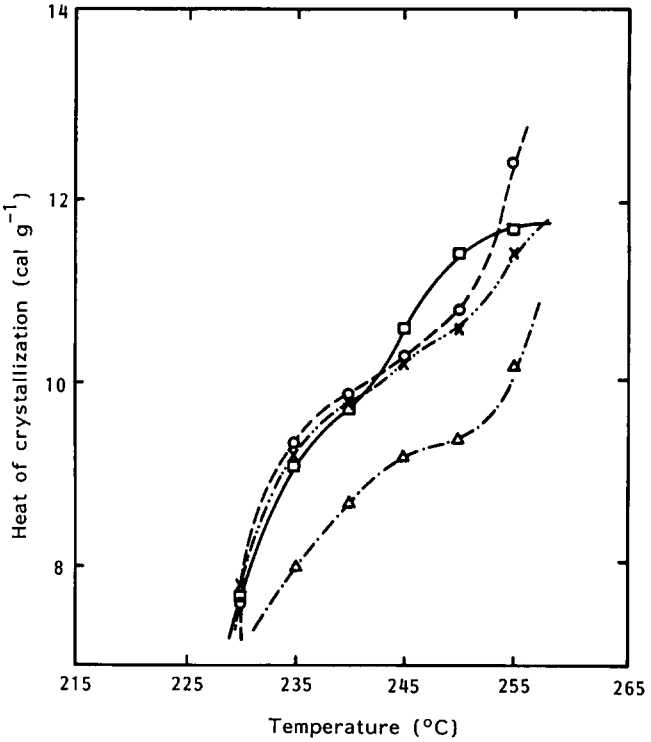

Figure 13 Heat of crystallization as a function of crystallization temperature corresponding to PPS materials with different endgroup counter-atoms. For meaning of symbols see *Figure 8*

phase in the polymer melt. These aggregates seemed to be the true nucleating species of the crystallization. For polycarbonate, Bailly *et al.*[7] reported that both nucleation and growth were affected by the presence of ionic chain ends. However, in these cases, there are chemical reactions occurring. PET and PC were shown to undergo a series of reactions including chain scission and chain rebuilding[6,7] that do not occur in PPS. Nevertheless, in none of these cases was the effect of the counter-ion studied.

We suspected that we might be able to note possible differences in endgroup association by studying the melt viscosity at low shear rates where Newtonian behaviour could be observed. To do so, of course, it was necessary to be above T_m and a temperature of 300°C was used. While, indeed, Newtonian or zero shear viscosity behaviour was obtained at low shear rates ($< 10\,s^{-1}$) by use of a Rheometrics, RMS, relatively small differences existed between the four materials, thereby nullifying the usefulness of this approach. However, the lack of differences may not be taken as absolute confirmation that endgroup association does not influence the crystallization process, but rather may simply be due to the excessive thermal energy (300°C) that limits the influence of ionic or coulombic interactions being observed. Hence, we cannot completely rule out the possibility of ionic aggregates influencing the crystallization behaviour (nucleation and growth) at lower temperatures.

Figure 13 displays the overall heat of bulk crystallization plotted as a function of crystallization temperature for samples crystallized from the melt. The usual increasing trend with increasing temperature is observed. PPSNa, PPSZn, and PPSCa present about the same values of ΔH_c as PPS that has not undergone ion-exchange treatment. However, PPSH has values of ΔH_c that are 15% lower, indicating that it crystallizes less than PPSNa, PPSZn and PPSCa. Legras *et al.*[6] and Bailly *et al.*[7] reported that the crystallinities of sodium carboxylate-terminated PET and sodium phenoxide-terminated PC largely exceeded the limiting values observed in the polymers that did not have the ionic endgroups. If the ionic character of the endgroup is considered as one of the factors regulating the attainable final crystallinity, it is reasonable to find PPSH with the lowest heat of crystallization, since PPSH would have the lowest ionic character of the endgroups in the samples studied. Indeed, we do not have any further explanation of the influence of the counter-atom on crystallization behaviour at this time. However, the results are quite reproducible. Further experimentation is required to acquire a better understanding of these results. Two variables seem to be of interest: (1) the effect of the ionic character of the endgroup-counter-atom bond; and (2) the effect of the oxidation state of ionic counter-atoms with similar ionic character on the crystallization behaviour of PPS.

CONCLUSIONS

The crystallization kinetics of poly(phenylene sulphide) were studied as a function of the branching agent content, and as a function of the chemical nature of the endgroup counter-atom. In both cases, the overall rate of bulk crystallization followed an Avrami equation with exponent $n \approx 3$. An increase in the branching agent content to 0.2 mol% produced a decrease in the overall rate of bulk crystallization by a factor of 5, a decrease in the growth rates by a factor of 2.2, and a decrease in the nucleation density by a factor of 3.5. In addition, the heat of crystallization was somewhat lower.

The chemical nature of the endgroup counter-atom affected the kinetic parameters in different ways. The growth rates could be arranged in decreasing order as follows: PPSCa > PPSH > PPSZn > PPSNa. However, the overall rates of bulk crystallization were, in decreasing order, PPSH > PPSZn > PPSCa > PPSNa. The nucleation densities determined the trends of the overall rate of bulk crystallization. In all cases, the nucleation densities were higher than those corresponding to PPS that had not undergone ion-exchange processes. As judged from the values of the heats of crystallization, the crystalline contents of PPSNa, PPSCa, and PPSZn were very similar to that of PPS that had not undergone the ion-exchange treatment. However, PPSH presented a value of the heat of crystallization 15% lower than can be rationalized by considering the ionic character of the endgroups.

ACKNOWLEDGEMENTS

The authors are grateful to Dr C. J. Stacy for sharing the well characterized samples used in this study, to Mr W. M. Whitte for supervising the rheological experiments and to the Phillips Petroleum Company for their financial support.

REFERENCES

1 Edmonds, Jr., J. T. and Hill, Jr., H. W. US Patent 3 354 129, 1967
2 Short, J. N. and Hill, Jr., H. W. *Chem. Tech.* 1972, **2**, 481
3 Hawkins, R. T. *Macromolecules* 1976, **9**, 189

4 Shue, R. S. *Dev. Plast. Technol.* 1985, **2**, 259
5 Campbell, R. W. US Patent 3 919 177, 1975
6 Legras, R., Bailly, C., Daumerie, M., Dekoninck, J. M., Mercier, J. P., Zichy, V. and Nield, E. *Polymer* 1984, **25**, 835
7 Bailly, C., Daumerie, M., Legras, R. and Mercier, J. P. *J. Polym. Sci., Polym. Phys. Edn* 1985, **23**, 751
8 Hill, Jr., H. W. *Ind. Eng. Chem. Prod. Res. Dev.* 1979, **18**, 252
9 Norton, D. R. and Keller, A. *J. Mater. Sci.* 1984, **19**, 447
10 Mandelkern, L., Glotin, M. and Benson, R. A. *Macromolecules* 1981, **14**, 22
11 Mandelkern, L. and Maxfield, J. *J. Polym. Sci., Polym. Phys. Edn* 1979, **17**, 1913
12 Kawai, T., Ujihara, K. and Maeda, H. *Makromol. Chem.* 1970, **132**, 87
13 Voigt-Martin, I. G., Alamo, R. and Mandelkern, L. *J. Polym. Sci., Polym. Phys. Edn* 1986, **24**, 1283
14 Strobl, G. R., Engelke, T., Maderek, E. and Urban, G. *Polymer* 1983, **24**, 1585
15 Maderek, E. and Strobl, G. R. *Colloid Polymer Sci.* 1983, **261**, 471
16 Banks, W., Gordon, M., Roe, R. J. and Sharples, A. *Polymer* 1963, **4**, 61
17 Strobl, G. R., Schneider, M. and Voigt-Martin, I. G. *J. Polym. Sci., Polym. Phys. Edn* 1980, **18**, 1361
18 López, L. C. and Wilkes, G. L. *J. Polym. Sci., Polymer Lett. Edn* 1986, **24**, 573
19 López, L. C. and Wilkes, G. L. *Polymer* 1988, **29**, 106
20 Stacy, C. J. *J. Appl. Polym. Sci.* 1986, **32**, 3959
21 Hoffman, J. D. and Weeks, J. J. *J. Res. Natl. Bur. Stds.* 1962, **66A**, 13
22 Avrami, M. *J. Chem. Phys.* 1939, **7**, 1103; 1940, **8**, 212; 1941, **9**, 177
23 Wunderlich, B. 'Macromolecular Physcis', Vol. 2, 'Crystal Nucleation, Growth, Annealing', Academic Press, New York, 1976
24 Jog, J. P. and Nadkarni, V. M. *J. Appl. Polym. Sci.* 1985, **30**, 997
25 Lovinger, A. J., Davis, D. D. and Padden, Jr., F. J. *Polymer* 1985, **26**, 1595